Journal of Basic and Environmental Sciences, 5 (2018) 174-186

ISSN
Online: 2356-6388
Print: 2536-9202

Research paper Open Access

The impact of hydrogeological setting on the protection of coastal groundwater aquifers, El Dabaa, Northwestern Coast, Egypt

[*]U. A. Abu Risha[1] and N. Sturchio[2]

[1]Geology Department, Desert Research Center;
[2]Department of Geological Sciences, University of Delaware, USA
[*]Corresponding author: osamaaborisha@gmail.com

Abstract

El Dabaa is located on the Northwestern Coast of Egypt. The main aquifers at El Dabaa are the Middle Miocene fractured limestone and the Pleistocene oolitic limestone. The hydrogeologic setting of these aquifers exposes them to various vulnerability degrees of contamination and salinisation. Seawater intrusion (SWI) and groundwater overpumping represent the main threats of the studied aquifers. This paper aims to provide practical solutions to protect the studied aquifers such as rainwater harvesting, artificial groundwater recharge, and the safe pumping of groundwater. Using the geographic information system (GIS), the sites suitable for implementing these measures were determined.

Keywords: Coastal aquifer, seawater intrusion, protection, GIS
Received; 5 May 2018, Revised form; 24 May 2018, Accepted; 24 May 2018, Available online 1 July. 2018

1. Introduction

The protection of coastal carbonate aquifers in arid regions against natural and anthropogenic threats, is a major challenge. Carbonate sediments and rocks are highly soluble in water. The existence of fractures in carbonate rocks facilitates their dissolution resulting in the development of cavities and other karst features. The hydrogeologic setting of fractures and karst carbonate aquifers is highly complicated. Groundwater in such aquifers flows predominantly in the fracture networks. The carbonate matrix itself has much lower hydraulic conductivities compared to the fracture network. Accordingly, fractured carbonates are mostly of dual porosity nature [1]. The dissolution of the carbonate matrix is controlled by the equilibria of carbonate minerals [2]. In coastal aquifers, seawater intrusion into the carbonate aquifers increases the dissolution of their matrices [3]. The interaction between the intruding seawater and carbonate aquifer groundwater imposes additional complexities on the hydrogeologic setting of these aquifers.

Coastal areas are usually in the center of the interests of tourism and industry investors. Many coastal areas represent centers of recreation and tourism resorts and villages. Such activities may result in environmental threats of different intensities including the contamination and deterioration of coastal aquifers. When such areas lack the required infrastructures and basic services, the intensities of the environmental issues exaggerate. The worseness of the situation is so strong in arid coastal areas where the replenishments of the aquifers are too limited to cope with the water demands. Sea level rise due to the increase of global temperature as a result of the greenhouse gas effects pushes the seawater intrusion deeper inland into the coastal aquifers imposing an additional threat of the water quality of these aquifers.

As the remediation of salinised and contaminated aquifers is either impossible or at least difficult, protection of aquifers from the groundwater deteriorating processes is a must. However, the protection measures of coastal carbonate aquifers are not an easy task. Protection measures are usually applied at different scales ranging from whole watersheds down to single water supply wells [4]. The best protection measures are those which are based on the comprehensive management of both surface and groundwater resources. For example, the harvest of storm water runoff that is lost to the sea in coastal aquifers in cisterns and surface reservoirs can ease the demand stress on the groundwater resources. In other areas, some of the runoff can be used to artificially recharge aquifers. The treated waste water in coastal areas can be used to create hydraulic barriers to limit the extent of the intruding seawater [5]. This paper aims at the assessment of the threats on the coastal carbonate aquifers at El Dabaa, Northwestern coast, Egypt and at providing solutions of the problems impacting the groundwater quantities and qualities using GIS and environmental tracer techniques.

2. Area of Study

The study area is located on the North-Western Coast of the Mediterranean Sea. It lies about 142 km west of Alexandria. It is easily accessible via highway roads and is also served by the El Alamain International Airport (Fig. 1). It is arid with average annual rainfall of about 164 mm. The rainfall generally occurs between October and March. December and January are the most humid months with monthly averages of 33 and 32.4 mm (1951–1992). The maximum average temperature over the period 1996–2008 is 22 °C in January and 31.6 °C in September. The minimum average temperatures are 7.2 °C in February and 23.7 °C in August, respectively [6]. The scarcity of rainfall and intense evaporation strongly impact groundwater recharge. Rrunoff ranges from 16.5 to 25 mm (10-15.3 % of rainfall; [6].

In the last three decades, many touristic resorts and villages have been constructed. The constructions of such villages and resorts continue until now. Most of these villages have been built on the oolitic limestone ridges which extend along the coast. These ridges represent the main fresh groundwater aquifer in the area. Large areas of these ridges have now disappeared underneath these villages and in some areas their rocks were cut into bricks used in the building of the villages.

The area has been subjected to many geological, geophysical, and hydrogeological studies (e.g. [6-15]. Such studies provide clear information about the hydrogeologic setting of the area.

Geomorphologically, the area can be subdivided into coastal plain (0-20 m.a.s.l) in the north, piedmont plain (20-50 m.a.s.l) in the middle and tableland (50-254 m.a.s.l) in the southwestern corner of the study area (Fig. 2). West of longitude 28.3º E the piedmont plain is very narrow whereas the coastal plain is almost absent. To the east of this longitude, the plains are wider and the plateau retreated southward. The geomorphic units are lithologically-controlled. The coastal plain is developed on Quaternary sediments; the piedmont plain is predominantly developed on soft Pliocene bedrock; whereas the tableland is developed on harder limestone of Middle Miocene. The coastal plain is dotted by elongated E-W ridges composed of oolitic limestone whereas the piedmont plain is dotted by remnant isolated hills of the tableland rocks. The drainage basins are shallow with low stream order. Generally, the slope in the area is gentle. It ranges between 0 and 15 ‰. The slope is greater along the coastal ridges and reaches about 200 ‰ [15].

Fig. (1): Location of study area and collected samples, El Dabaa, Northwestern Coast, Egypt

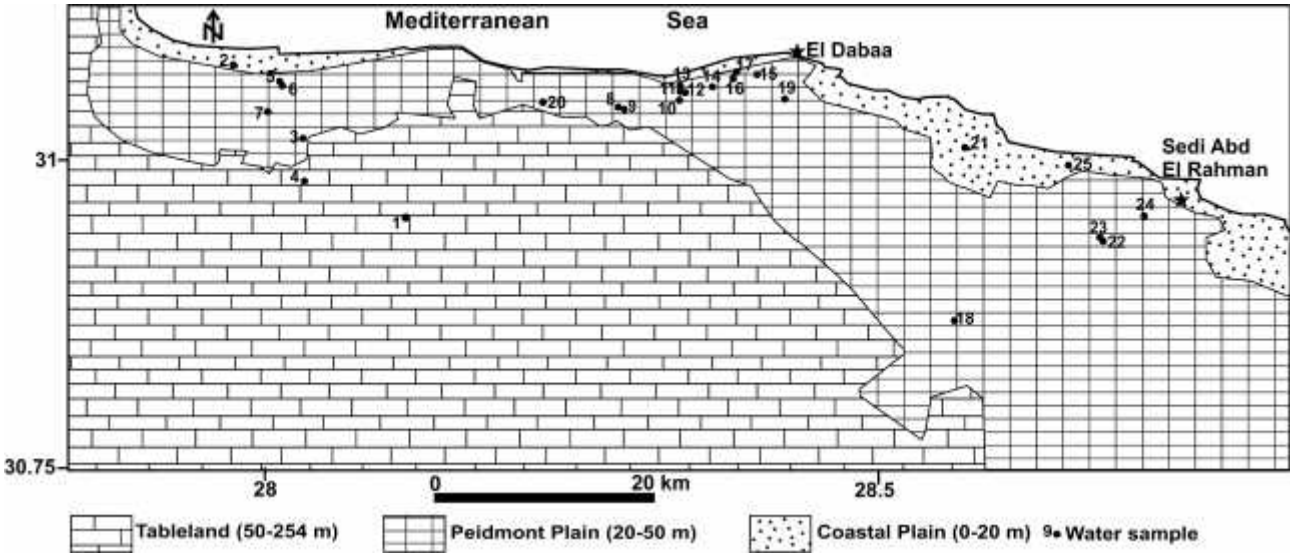

Fig. (2): Geomorphologic map of El Dabaa, Northwestern Coast, Egypt

Stratigraphically, the rocks exposed in the study area were deposited in the Middle Miocene, Pliocene, Pleistocene and Holocene (Fig. 3). The Middle Miocene rocks form Marmarica Formation which consists of fractured and karst limestone intercalated with clay and marl interbeds. The thickness of the Marmarica Formation in the area of study is about 180 m [9]. The Pliocene rocks are represented by El Hagif Formation that is composed of creamy limestone on top and brown calcareous sandstone at base. The Pleistocene sediments are represented by the oolitic limestone which forms coastal ridges. The Holocene sediments consist of a variety of deposits including beach, aeolian, lagoonal, and alluvial sediments (Fig. 4).

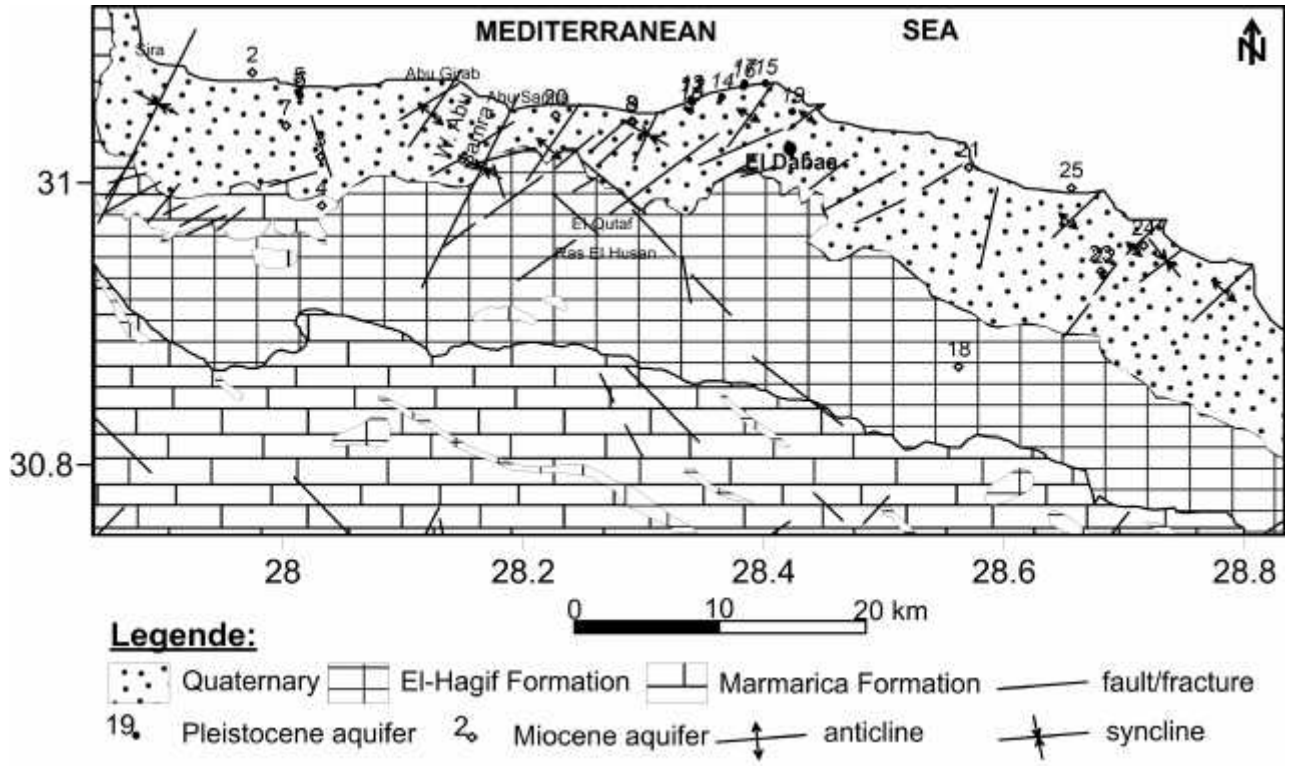

Fig. (3): Geologic map of El Dabaa, Northwestern Coast, Egypt [16]

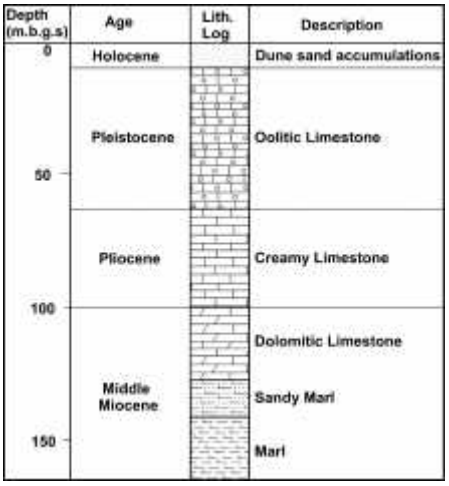

Fig. (4): Idealized stratigraphic section at El Dabaa area [7]

Structurally, the gulfs along the Mediterranean coast represent synclines whereas the heads (such as El Dabaa) represent anticlines (Fig. 3). These structures strike NE. The study area is a part of the Marmarica Homocline, which occupies the area north of the Quattara Depression [17]. El Dabaa area is underlain by Miocene strata that dip north at 10-20° and are unconformably overlain by Pleistocene oolitic limestones. Local structural undulations are present in the form of gentle up fold and down fold structures, broad monocline structures and unconformities [17]. According to El Shamy [7], the area is affected by two monoclinal structures oriented in the NE-SW direction. Between the two structures is a local synclinal basin which is underlain by cream-coloured Pliocene limestone (Fig. 3). Two synclinal basins, doubly plunging synclines, are known in the El Dabaa area; Fuka syncline and Qutaf syncline. The Fuka doubly-plunging syncline lies between the Sira monocline to the west and Ras Abu Girab-Abu Samra monocline to the east. It is occupied by alternating beds of Middle Miocene limestone and clay [18]. The Qutaf syncline lies between the eastern edge of Ras Abu Girab-Abu Samra monocline and the Sira monocline and has the same orientation as the Fuka syncline. Most of the folded structures are oriented NE-SW [17].

According to Abd el-aal et al. [19], two sets of joints affect the Miocene lithologies, one strikes E-W and the other strikes due north. These sets do not exist in the Pleistocene lithologies, which limits the timing of joint formation in the Miocene strata between the Middle Miocene and Pleistocene. However, three surface microfracture sets were detected in the Pleistocene oolitic limestone ridges at El Dabaa [10] (Fig. 5a). The lengths of these fractures vary between 10 cm to more than 1 meter. The widths of the opening of these fractures vary between less than 1 mm, to about 1cm in some fractures. These fractures are without displacement or filling. The great, majority of them have a dip between 70 and the vertical. The trend of the fractures in core samples from these ridges is NNE-SSW direction (Fig. 5b). The statistical analysis of the surface lineaments mapped by [16] shows that the NE-SW structural lineaments are dominant and followed by the NW-SE ones (Fig. 5c). Most of these lineaments reflect the fracturing of the Marmarica Limestone.

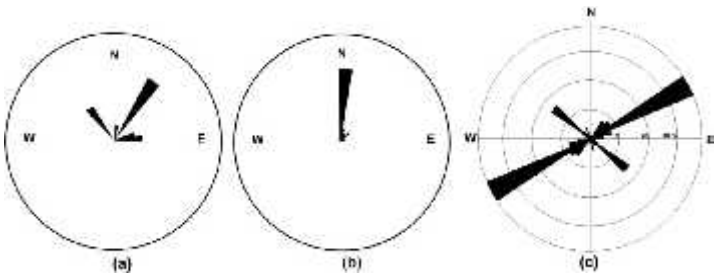

Fig. (5): Rose diagrams of: (a) surface and (b) subsurface (core samples) fractures of second ridge [10], and (c): surface lineaments [16]

No faults were detected in the subsurface in the northeastern part of the area [13]. Nevertheless, E-W step faults were recorded in the subsurface to the west of El Dabaa [20]. Two major faults are reported in the area around El Dabaa [21]. One strikes NW-SE and is revealed in geophysical studies east of Ras El Hekma [8]. The second fault has the same trend and is documented through field observations east of the Ras Abu Girab–Abu Samra monocline. The downthrown side of this fault is due north; with displacement ranging from 8 to12 m. Subsurface major E-W faults throwing towards the north are also expected [17].

3. Hydrogeologic Setting

There are two main aquifers at El Dabaa; the Pleistocene and the middle Miocene aquifers. The fractures and other structures facilitate the replenishment of these aquifers from the local precipitation. The following sections provide a description of the hydrogeologic setting of each of these aquifers.

3.1. Pleistocene oolitic limestone aquifer

This aquifer has a wide distribution and considered to be the most important aquifer along the coastal strip. It extends about 10 km southward. The foreshore oolitic limestone ridges are characterized by less cementing materials compared to the inland ridges. The flanks of the ridges are covered by loose foreshore sand accumulations, which permit a direct infiltration and percolation of rainfall. The groundwater exists as a free water table (phreatic condition). The groundwater table in this aquifer attains altitude close to the mean sea level. It is a result of the local percolation in the coastal plain and the inflow from sea water. The horizontal flow from the sea forms a saline water table overlain by a fresh water sheet. Such thin sheet of the fresh water is a result of natural balance between the surplus of recharge from precipitation and the discharge through seepage to the sea [18]. The geophysical studies show that the upper part of the oolitic limestone represents the shallow aquifer in this area. This aquifer can be distinguished into two zones. The upper zone is the brackish, while the lower one is saline due to salt-water intrusion [13].

At Ras El Hekma (the west of the area of study), the investigated aquifer is characterized by permeability (0.0015 m/min), Transmissivity (0.03 m^2/min) and storativity ($6.31*10^{-6}$) [22]. At El Dabaa locality, the direction of groundwater flow in this aquifer is due north and south. The hydraulic gradient is gentle in the northern part (0.0002), while at the southern one it records (0.0003), [23].

3.2. Miocene Fractured Limestone aquifer

The Marmarica aquifer is composed of limestone, dolomite and shale sequence related to the Middle Miocene. This formation is largely fractured and exists in successive horizons separated by impervious clays with occasional bands of sandstone. The groundwater in this aquifer exists in the form of thin sheets accumulating at the contact with the impervious clay and depends mainly on its supply by local rainfall (semi confined water). The depth to water ranges from 10.6 (well 21) to 63 (well 3) m (Table 1). The groundwater of the Marmarica aquifer is naturally discharged by subsurface flow into the Mediterranean. The middle Miocene aquifer contains two water-bearing zones. The upper zone is composed of white chalky limestone, while the lower unit is built of marly limestone [15]. The lateral and vertical facies changes affect the productivity of the aquifer, particularly along the coastal area. The estimated transmissivity of this aquifer ranges from 2.15 to 4.8 m^2/d [24].

4. Methods

The protection of groundwater aquifers requires an understanding of their hydrogeologic setting and the possible processes that may threat their groundwater quantity and quality. In order to determine such processes, twenty four groundwater samples were collected from the Pleistocene (11 samples) and Middle Miocene (12 samples) aquifers in the area of study. A sample was collected from a deep well that discharges mixed groundwater from the Lower Miocene and Middle Miocene aquifers (Sample No. 4). A rainwater sample was collected from a small pool formed after a rainstorm. This sample can be regarded as a recharge water representative. A seawater sample was also collected from the Mediterranean at El Hammam City. Temperature, pH, electric conductivity, and depth to water table were measured in situ for each of the collected samples (Table 1). The samples were analyzed to determine the concentrations of major ions and trace elements. The measured concentrations of some ions and elements were used as tracers of seawater intrusion in the studied aquifers. The samples were analyzed at the laboratories of the Desert Research center, Egypt. The detailed analyses procedures are described elsewhere [e.g., 25]. Sites of rainwater harvesting and artificial recharge measures were determined using the flood simulation in ARC GIS.

Table (1): Key parameters and field measurements of the studied water points (January 2016)

No	Aquifer	DFC[x] (km)	Elevation (m.a.s.l)	TD (m)	DT W (m)	W.L (m.a.s.l)	E.C mmohs/cm	pH	T (°C)
R	Rainwater			-	-	-	179.7	8.	15.
2	M. Miocene	1.45	32	38	-	-	48200	7.	24.
3	M. Miocene	7.56	38	77	63	-25	29700	7.	24
4	L & M Mio[+]	11.4	67	300	75.2	-8.2	21800	7.	22.
5*	Pleistocene	2.6	35	42	36.2	-1.26	4080	8	18.
6	Pleistocene	2.87	44	-	35.5	8.44	9970	8.	21.
7	M. Miocene	5.57	27	35	-	-	23100	8.	14.
8^	M. Miocene	3.25	44	34	-	-	6660	8	23
9	M. Miocene	3.25	41	34	28.4	12.56	3430	8.	21.
10	Pleistocene	2.11	25	22.	21.2	3.76	2910	9.	21.
11	Pleistocene	1.4	21	17.	17.2	3.75	4250	7.	21.

12	Pleistocene	1.5	20	-	-	-	2520	7.	21.
13	Pleistocene	1.22	19	-	18.5	0.5	4030	8.	22.
14	Pleistocene	1.85	20	-	21.7	-1.76	6850	7.	21.
15	Pleistocene	1.34	16	-	17	-1	5630	8.	21.
16	Pleistocene	1.6	15	-	18.3	-3.39	5760	8.	21.
17	Pleistocene	1.34	13	-	18.2	-5.27	8300	8.	20.
18	M. Miocene	19.8	44	40	37	7	6190	7.	21.
19	Pleistocene	4.17	31	-	24.0	6.92	1920	7.	20.
20	M. Miocene	2.83	38	68	37.8	0.14	20600	7.	21.
21	M. Miocene	3.38	13	13.	10.6	2.38	5540	7.	20.
22	M. Miocene	7.43	33	150	29.7	3.3	37500	8	21.
23	M. Miocene	7.23	30	190	29.4	0.54	37300	7.	21.
24	M. Miocene	4.62	17	15	14.7	2.27	46400	8.	20.
25	M. Miocene	0.89	17	17	13	4	13150	8.	21
S	Seawater[#]	0	0	-	-	0	59800	8	24.

*In an area irrigated from drinking water pipeline; salinity increasing strongly with pumping
+ Lower and Middle Miocene # Mediterranean Seawater at Hammam City
^ Sample color is white like milk x distance from coast (DFC) - not measured or estimated

5. Results

The analyses results of the concentrations of major ions and trace elements in the collected water samples are given in Tables 2 and 3, respectively. The groundwater total dissolved solids (TDS) of the Pleistocene and Miocene aquifers range from 1002 (No. 19) to 5900 (No. 6) and from 2307 (No. 9) to 34332 mg/l (No. 24), respectively. The groundwater chloride concentrations in these aquifers range from 437 (No. 19) to 3188 (No. 6) and from 668 (No. 9) and 20310 mg/l (No. 24), respectively. These wide ranges of salinity reflect complicated salinization processes including the evapoconcentration of recharge water, the interaction with aquifer rocks, and mixing with intruding seawater. The evapoconcentration strength depends on the prevailing climatic conditions during recharge. In arid regions, such as the study area, this process can dominate the other salinization processes especially in sandstone aquifers [26].

Table (2): Major ion concentrations (mg/l); January 2016

No	Ca	Mg	Na	K	CO_3	HCO_3	SO_4	Cl	TDS	Mg/Ca^	SR*
RW	18.9	3	10	3	0	15.3	31.2	25.	99.4	0.26	1.69
2	364	684	110	2	18	134	830	200	3325	3.1	131.
3	573	538	600	9	15	177	3338	977	2041	1.55	50.9
4	563	419	360	8	15	119	925	745	1311	1.23	55.6
5	161	117	530	1	30	226	242	106	2275	1.2	4.17
6	133	163	185	6	12	211	383	318	5900	2.03	14.3
7	505	518	400	1	33	82	22	858	1382	1.69	74.4
8	216	91	120	2	15	153	1149	167	4447	0.69	9.98
9	86	40	650	2	15	204	725	668	2307	0.77	3.05
10	13	11	610	1	45	418	164	566	1632	1.35	1.22
11	70	130	620	2	60	415	104	114	2359	3.06	2.41
12	127	87	220	1	36	293	17	643	1291	1.14	1.95
13	59	111	600	4	45	314	352	964	2330	3.1	2.68
14	57	189	114	4	66	244	325	190	3844	5.44	6.14
15	41	117	940	4	48	393	102	162	5440	4.74	3.67
16	52	142	100	4	105	458	53	173	3359	4.48	3.09
17	39	232	145	4	141	689	77	244	4768	9.72	2.94
18	220	164	840	3	42	204	730	154	3678	1.23	6.26
19	39	41	270	2	21	271	37	437	1002	1.75	1.49

20	174	299	480	8	21	156	1017	745	1392	2.83	42.2
21	345	130	780	3	24	271	1665	900	4010	0.62	3.05
22	309	516	860	1	24	79	649	143	2468	2.76	139.
23	516	532	840	1	18	131	455	153	2547	1.7	103.
24	387	698	114	1	24	92	1298	203	3433	2.97	175.
25	194	237	320	5	42	183	1776	462	1022	2.01	20.5
SW	446	1437	106	4	18	85	3618	175	3421	5.32	170.

*SR is Simpson ratio; Cl/(CO_3+HCO_3) concentrations in mg/l [27], ^ molar ratio

The role of water-rock interactions is more important in carbonate aquifers. The importance of this process increases with the existence of gypsum and/or other evaporites in the carbonate matrix. Seawater intrusion (SWI) occurs in coastal aquifers. Its depth into an aquifer depends on its type, porosity, and depth. This process represents the main groundwater salinization process in most coastal aquifers that experience overpumping. The following section discusses the impacts of the different salinization processes affecting the groundwater quality and proposes some measures to limit them.

5.1. Evapoconcentration

The impact of evapoconcentration on recharge water is well documented [e.g., 28]. In arid zones, the impact of evapoconcentration on the salinity of recharge water is often strong [26]. The stable isotope contents of El Dabaa groundwater from both the Pleistocene and Miocene aquifers show that this water is recharged from local rainfall ([11]; [15]). However, Yousif et al. [15], using the isotope signatures, could determine groundwater samples mixed with Nile water from a pipeline conveyed to Matruh for drinking. Some farmers use this water for irrigation where some of it infiltrates and reaches the aquifers. The positive correlation between the Cl and O-18 concentrations measured by these authors in samples not mixed with Nile water (Fig. 6) reflects an evapoconcentration impact on groundwater salinity at El Dabaa.

Table (3): Trace element concentrations, January 2016

No	Al	B	Ba	Fe	Li	Mn	Sr	Zn
RW	0.642	0.06	nil	0.29	0.003	0.002	0.11	
2	0.082	5.648	nil	0.004	0.242	0.0002	22.68	nil
3	0.115	3.783	0.003	2.575	0.237	0.059	13.93	0.016
4	0.129	2.474	0.007	4.88	0.156	0.121	11.3	0.317
5	1.681	0.639	0.034	1.682	0.044	0.054	30.19	0.573
6	0.648	2.293	0.022	0.577	0.068	0.015	15.23	0.24
7	0.197	4.55	0.009	0.145	0.158	nil	12.87	0.069
8	4.39	1.681	0.014	2.68	0.058	0.069	5.998	0.018
9	0.092	1.085	nil	0.054	0.032	nil	3.965	0.0002
10	0.529	3.245	0.018	0.373	0.026	0.004	2.44	0.163
11	0.096	1.077	0.098	0.156	0.04	0.008	11.58	0.111
12	0.131	0.29	0.114	0.105	0.021	0.014	5.327	0.108
13	1.877	2.582	0.038	0.993	0.05	0.032	21.72	0.17
14	0.591	1.81	0.016	0.358	0.068	0.004	25.37	0.088
15	0.363	2.013	0.063	0.501	0.043	0.033	14.42	0.086
16	0.356	1.207	0.081	0.514	0.047	0.101	19.02	0.1
17	0.01	1.129	0.097	0.006	0.069	nil	17.34	0.022
18	0.08	0.945	0.053	0.107	0.128	0.03	8.717	0.122
19	0.158	0.957	0.051	0.085	0.029	nil	2.777	0.086
20	2.248	5.385	0.027	1.451	0.104	0.034	12.6	0.129
21	2.067	3.149	0.013	0.976	0.072	0.097	6.579	0.193
22	1.079	2.928	0.043	0.629	0.14	0.039	6.814	0.205
23	2.165	3.088	0.073	1.497	0.157	0.289	9.567	0.258
24	2.993	3.8	0.061	1.821	0.197	0.12	10.29	0.283
25	4.166	5.649	0.046	3.632	0.069	0.072	4.379	0.805
SW	nil	5.164	0.001	0.0005	0.194	nil	7.538	

5.2. Water-Rock interactions (WRI)

The concentration of CO_3 in the Pleistocene and Miocene aquifers ranges from 30 (No. 5) to 141 (No. 17) mg/l and from 15 (No. 3, 8, and 9) to 42 (No. 18 and 25) mg/l, respectively (Table 2). Only two Pleistocene groundwater samples have low CO_3 concentrations (No. 6 and 19). The higher CO_3 concentration in the Pleistocene

aquifer compared to the Miocene aquifer can be attributed to the higher $CaCO_3$ content of the Pleistocene oolitic limestone [9]. The Miocene fractured limestone is harder and dolomitic in some places. Accordingly, it is less soluble than the younger oolitic limestone. Moreover, the carbonate solubility increases with increasing the availability of CO_2. As groundwater in the Miocene aquifer is generally deeper than in the Pleistocene aquifer, the concentrations in the Miocene aquifer of the carbon species are lower than their concentrations in the Pleistocene aquifer (Table 2). The highest HCO_3 concentrations exist in the groundwater with low salinity in the Pleistocene aquifer which also reflects recent recharge from local rainfall. Also, Sr has relatively low concentration in seawater (7.5 mg/l; Table 3). Carbonate rocks are rich in Sr. Hence, the increase of Sr in groundwater can be attributed to carbonates dissolution (e.g., samples 2, 5, 13, and 14). Many of the Pleistocene aquifer samples have high Sr concentrations compared to the Miocene aquifer which can be attributed to the higher solubility of the oolitic limestone of the Pleistocene aquifer compared to the hard limestone of the Miocene aquifer.

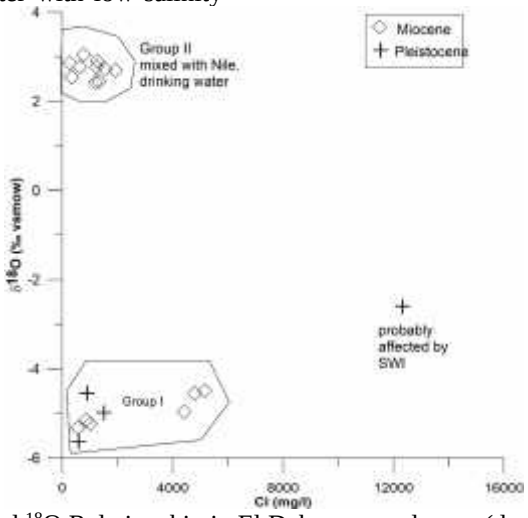

Fig. (6): Cl and ^{18}O Relationship in El Dabaa groundwater (data after [15])

5.3. Seawater Intrusion (SWI)

Seawater intrusion (SWI) is a global coastal phonemenon. It has been the focus of many studies worldwide [29]. Nevertheless, the occurrence of SWI in the area of study and its surroundings is a matter of debate between researchers. Based on hydrochemical evidences, some researchers believe that (SWI) occurs in these areas to different degrees (e.g., [12, 14, 30, 31, 32]). Other researchers see that the SWI does not affect the groundwater salinity (e.g. [15, 33]). They attributed the groundwater salinisation to the dissolution of aquifer carbonates and gypsum. However, some geophysical studies show fresh water layer floating on saline water layer (e.g., [13, 34]). Awad et al. [11] have attributed the high tritium content of some samples to mixing with sabkha water or seawater. Ibrahim [20] recommended no drilling of water wells deeper than 20 m to avoid the impact of the seawater encroachment. The threat of SWI will be vital in case of the construction of the proposed nuclear power plant as any leaked nuclear material can be transported to the aquifers by the intruding seawater.

There is an increase of groundwater salinity with decreasing the level of water table. This relationship is quite clear in the case of the Pleistocene aquifer. The samples with water table lower than sea level have greater salinities compared to the wells with water levels higher than sea level (Fig. 7a). In the Miocene aquifer, the relationship is applicable to wells 3, 4, and 21 (Fig. 7b). The wide range of salinity within a narrow range of water levels higher than the sea level in this aquifer reflects the impact of upconing of saline water due to overpumping (wells 20, 22, 23, 24, and 25). Also, the penetration of the lower saline water layer in Wells 22 and 23 which have total depths of 150 and 190 m, respectively, is beyond the increase of salinity in these wells. Well No. 5 in the Pleistocene aquifer is 42 m deep. It ends 7 m below the sea level. It seems that the owner avoids overpumping to prevent the upconing of saltwater. Salinity also increases towards the coast (Fig. 8). Such relationship can be attributed to: (1) the gradual dissolution of aquifer minerals as the groundwater flows towards the coast; and (2) the increasing effect of SWI.

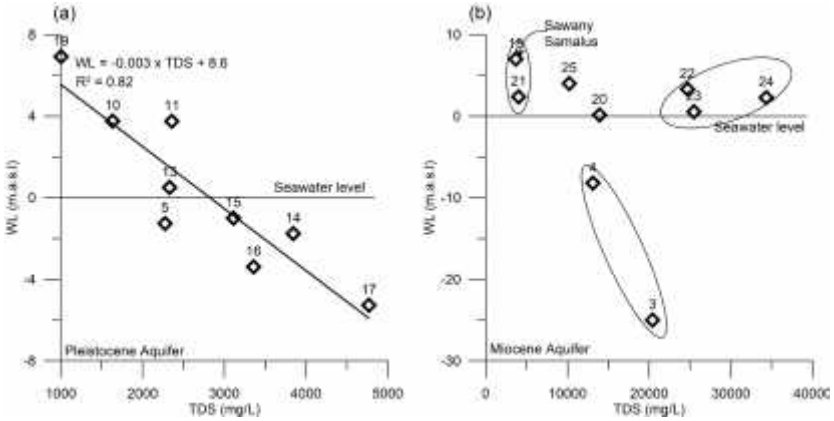

Fig. (7): The relationship between groundwater level and salinity

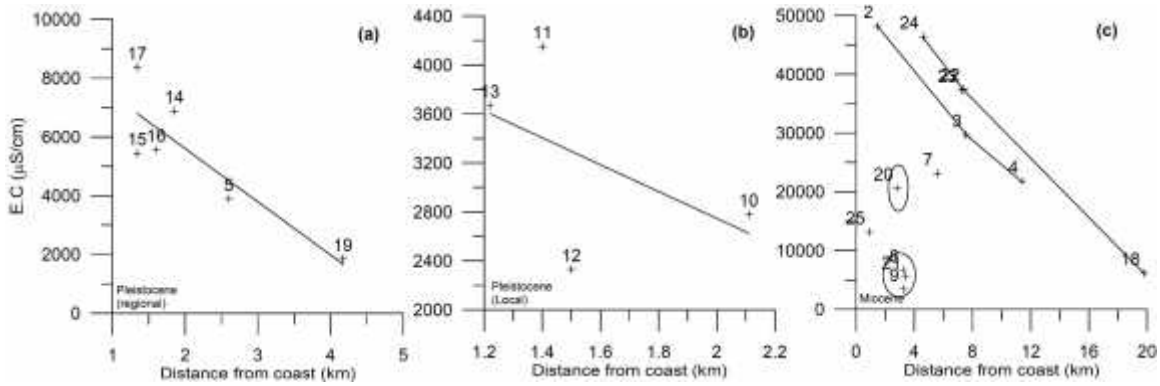

Fig. (8): Relationship of groundwater electric conductivity and distance from coast

The Mg/Ca ratio can be regarded as one of the best tracers of SWI because of the excess of Mg in seawater compared to Ca (Mg/Ca molar ratio = 5.3). Contrarily, Mg shows deficit in carbonate rocks and groundwater compared to Ca where the Mg/Ca ratio is mostly <1 (e.g, [9]). In rainwater accumulated on ground surface (RW; Table 2), this ratio is 0.26. There is a direct relationship between the Mg/Ca ratio and groundwater salinity (represented as Cl) in the studied aquifers (Fig. 9). As the Mg/Ca ratio in the aquifer carbonate rocks is <1, the increase of this ratio to levels >>1with increasing groundwater salinity can be attributed to either seawater intrusion or salt water upconing.

The Simpson ratio [27] has been extensively used as an indicator of SWI (e.g., [35, 36]). It is defined as: $Cl/(CO_3+HCO_3)$ with all concentrations are in mg/l. It is very high in seawater and low in continental groundwater. The measured SR in seawater is 170.1 whereas the ratio of the rainwater is 1.69 (Table 2). Sample 24 has identical ratio to that of seawater. In fact, the chemistry of this sample is quite similar to the seawater chemistry. Other samples that have SR approaching that of seawater are 2, 22, and 23. These samples are strongly affected by SWI. Samples 3, 4, 7, and 20 are strongly also affected by SWI. According to Simpson classification [27], sample 10 is slightly affected by SWI, samples 11, 12, 13, and 19 are moderately affected, samples 5, 9, 14, 15, 16, 17, 18, and 21 are injuriously affected, whereas the other samples which has SR greater than 15.5 are highly affected.

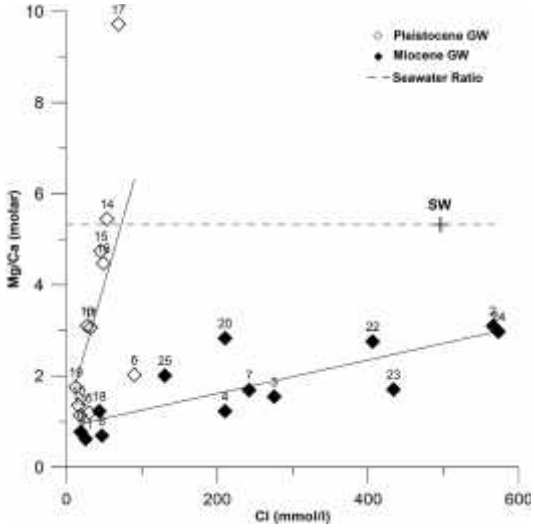

Fig. (9): Ralationship between salinity (as Cl concentration) and Mg/Ca molar ratio

Some trace elements can be used to trace SWI. For example, boron is abundant in seawater (5.2 mg/l; Table 3). Groundwater usually contains less boron concentration. The groundwater samples with boron concentrations comparable to that of seawater are expected to be affected by SWI (e.g., samples 2, 7, 20, and 25). Lithium occurs at low concentrations in carbonate rocks but has high concentrations in seawater. Accordingly, samples with high lithium concentrations approaching that of seawater are also expected to be affected by SWI (e.g., samples 2, 24, and 23).

6. Measures to protect aquifers

Aquifer protection can be partially done by measures capable to limit the impacts SWI and evapoconcentration. The impact of the latter can be awakened by harvesting rainwater in recharge pools, exposing the fractured bedrock to facilitate recharge, and preparing the recharge area for the recharge season. This requires the determination of the recharge season, the amount of rainfall required to trigger recharge, and the recharge rates. A monitoring system of recharge, groundwater salinity, and water level is essential to measure the success of the measures taken. The impact of SWI can be done by a variety of measures and techniques. The following section focuses on the management of aquifer recharge and SWI.

6.1. Increasing groundwater recharge

Increasing groundwater recharge requires the determination of the source and rate of recharge and the available surface runoff and other sources of water that can be used in recharging the aquifer.

6.1.1. Source of recharge

Comparing the groundwater stable isotope concentrations [15] to those of local rainfall [37], it can be concluded that the recharge occurs from local rainfall. The rainfall amount required to trigger recharge incidents ranges from 60 to 120 mm (Fig. 10). At Alexandria, such events occurred 26 times between 1961 and 2004 (43 years; i.e. once per ~ 1.7 years).

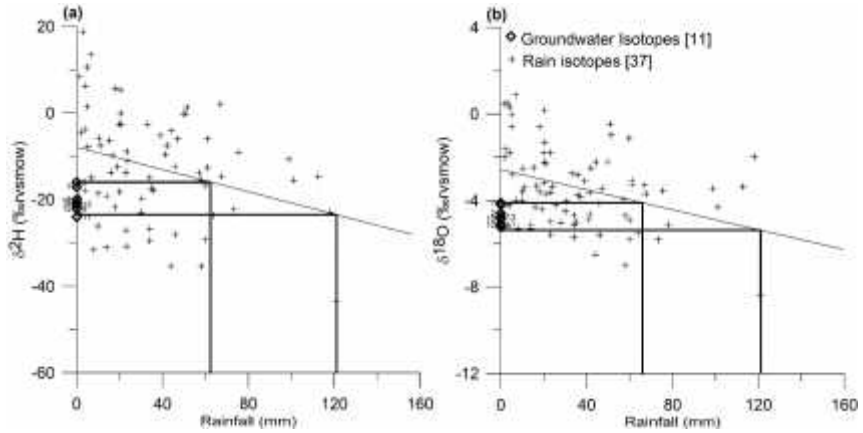

Fig. (10): Relationship between rainfall amount and its deuterium (a) and oxygen-18 (b) contents at Alexandria. Also plotted are the isotopic signatures of El Dabaa groundwater.

6.1.2. Recharge rates

Recharge rates can be estimated using the following chloride mass balance (CMB) steady state model which is widely used worldwide [38].

$$R = Cl_pP/Cl_g$$

where R is the average recharge rate (mm/yr), Cl_p is the average Cl concentration in atmospheric precipitation (wet and dry fallouts) (mg/l), Cl_g is the groundwater Cl concentration in (mg/l), and P is the mean annual rainfall in mm/year.

The maximum estimated recharge rate of the studied samples using the CMB is 4.5 mm/y which represent 2.75 % of the annual rainfall of 164 mm/y. The maximum estimated runoff is 25 mm/y or 15.3 % of the annual rainfall [6]. Accordingly, runoff is five times more than the recharge rate. Most of the runoff is lost to the sea. It is recommended to use runoff in increasing groundwater recharge via harvesting it in recharge dams, lakes, and injection wells. This is best done in areas with shallow fractured bedrocks in uncultivable lands especially in the southern part of the area of study.

Using the flood simulation capability in ARC GIS and the digital elevation model [39], the sites of floodwater accumulation, which are suitable for the different rainwater harvesting and artificial recharge measures, were determined (Fig. 11). Roads can also be used as means of rainwater harvesting by directing their slopes towards rainwater pipelines installed under the road sides with openings in the sides of the pavements.

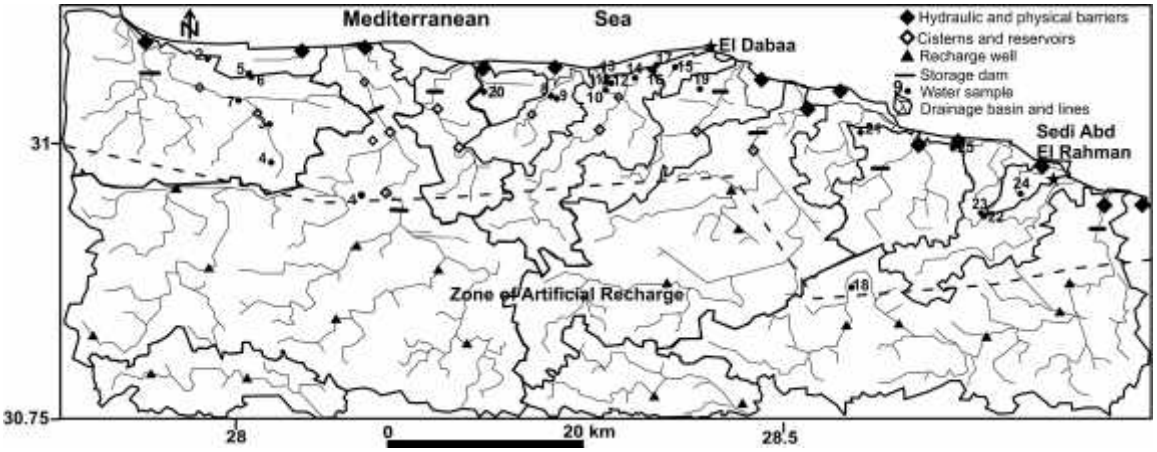

Fig. (11): Proposed locations of recharge wells, cisterns, and storage dams

6.2. Limit the impact of SWI

In the Pleistocene aquifer, there is a gradual increase of mixing with seawater with pumping and consequent lowering of water level. Decreasing the pumping rates is quite important to avoid such mixing. The depth to water in this aquifer ranges from 17 to 36.25 m.b.g.s (Table 1) and the thickness of the low salinity groundwater layer ranges from 6 to 24 m [13]. In such setting, scavenger wells can be used [40]. These wells may be drilled as a single borehole (Fig. 12-A) or as twinned boreholes (Fig. 12-B). They are equipped by two pumps. One extracts water from the fresh water layer whereas the other extracts from the underlying saline water layer. The concept of a scavenger well relies on the fact that interface upconing is the result of pumping in the freshwater zone while interface downconing of the fresh water layer is caused by pumping saline water. These two processes can be balanced by varying the pumping rates from the two zones. The pumped saline water from wells in the coastal zone can be disposed into the Mediterranean (e.g. wells 21, 24, and 25). In inland areas, the pumped saline water can be used in fish farming.

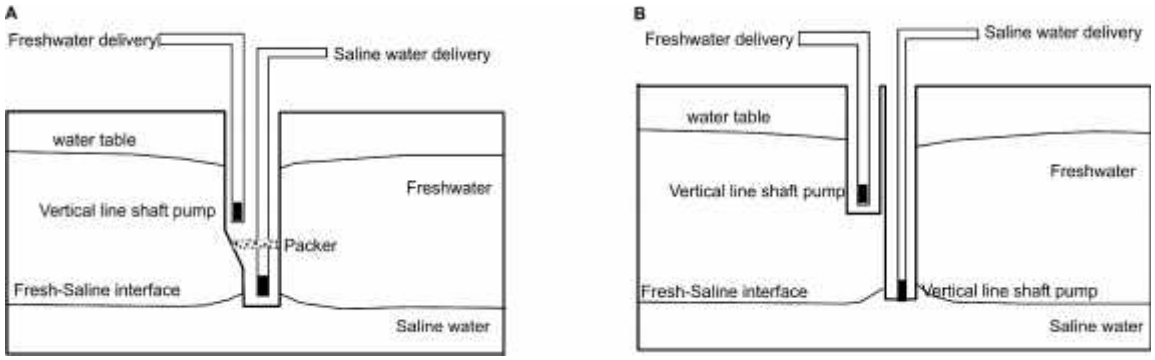

Fig. (12): Single borehole (A) and twinned borehole (B) scavenger well designs

In addition, artificial recharge schemes and the installation of injection wells can counteract SWI. The construction of extraction, injection, subsurface, and biological barriers can limit to some degree the inland advance of the intruding seawater [41, 42]. Injection barriers can be developed by either direct injection wells or by spreading basins. The water required for the hydraulic barriers cannot be derived from harvested rainwater. Instead, it should be derived from the treated waste water that results from the domestic, agricultural, and touristic usages. Hydraulic and physical barriers should be constructed along the coastline.

6.3. Prevention of random drilling

Shallow drilling only suits the hydrogeologic setting at El Dabaa. The best drilling depths in the Pleistocene and Miocene aquifers range from 13 to 40 m.b.g.s., depending on the ground elevation of the drilling sites. Hammer drilling has been extensively used to drill wells in the area of study. Some of these wells are deeper than they should be as they penetrate deep clay interbeds and layers with saline groundwater. As a result, many of the wells are abandoned as they extract saline water.

6.4. Convey more Nile water for drinking

Nile water is already conveyed to Matruh passing through El Dabaa. Some farmers use some of this water not only for drinking but also for irrigation although this act in illegal. If the quantity of water of this pipeline is increased and the residents of El Dabaa and the tourism resorts will be allowed to use it for drinking, the stress on the groundwater aquifers will be eased greatly. Moreover, the waste water results from the different uses will increase. This water can be treated and injected in the aquifer along the coastline to create hydraulic barriers which will reduce the impact of SWI.

Conclusions and recommendations

The main sources of groundwater salinisation at El Dabaa are evapoconcentration of solutes in recharge water and direct SWI or upconing of saline water as a result of overpumping. The interactions with aquifer rocks have weaker impact on the overall groundwater salinities in the studied aquifers. Recharge management can reduce the effect of evapoconcentration by rainwater harvesting in recharge pools, dams, or wells. The impact of seawater intrusion can be opposed by the means of hydraulic barriers that can be built up using treated wastewater. The upconing of saline water during pumping can be reduced by decreasing the pumping rates and the use of scavenger wells. Stopping random drilling is a must to protect the aquifers.

References

[1] P.G. Cook, A guide to regional groundwater flow in fractured rock aquifers, CSIRO Land and Water, Glen Osmond, South Australia, 2003.

[2] C.A.J. Appelo, D. Postma, Geochemistry, Groundwater and Pollution, second ed., A.A. Balkema, Leiden, The Netherlands, 2005.

[3] G.T. Chae, S.T. Yun, S.M. Yun, K.H. Kim, C.S. So, Seawater–freshwater mixing and resulting calcite dissolution: an example from a coastal alluvial aquifer in eastern South Korea, Hydrological Sciences Journal, 57-8 (2012) 1672–1683.

[4] N.S. Robins, P.J. Chilton, J.E. Cobbing, Adapting existing experience with aquifer vulnerability and groundwater protection for Africa, J. African Earth Sci., 47 (2007) 30–38.

[5] R.Jr. Luyun, K. Momii, K. Nakagawa, Effects of Recharge Wells and Flow Barriers on Seawater Intrusion, GROUND WATER, 49-2 (2011) 239–249.

[6] M. Yousif, O. Bubenzer, Geoinformatics application for assessing the potential of rainwater harvesting in arid regions. Case study: El Daba'a area, Northwestern Coast of Egypt, Arab. J. Geosci., 8 (2015) 9169–9191.

[7] I.Z. El Shamy, The geology of water and soil resources in El Dabaa area Western Mediterranean coastal zone U.A.R, M.Sc. Thesis, Fac. Sci, Cairo Uni. (1968).

[8] F.A. Hammad, The geology of soil and water resources in the area between Ras E l Hekma and Ras Alam El Rum, Western Mediterranean Littoral Zone, Egypt, Ph.D. Thesis, Fac. Sc., Cairo Uni. (1972).

[9] R.F. Misak, Geomorphology and geology of the area between El Daba'a and Ras El-Hekma, Western Mediterranean coastal zone, Egypt, M.Sc. Thesis, Fac. Sci., Ain Shams Uni. (1974).

[10] E.A. Eweida, L.A. Fayed, A.M. Abu El Ela, Fracture Permeability at El Dabaa Nuclear Power Plant Site, North Western Desert, Egypt, Egypt, J. Geol., 37-1 (1993), 77-90.

[11] M. Awad, F. Hammad, A. Aly, M. Sadek, Use of environmental isotopes and hydrochemistry as indicators for the of groundwater resources in El-Dabaa area, northwestern coastal zone of Egypt, Environ Geochem Health, 16 (1994) 31–38.

[12] M.A. Gomaa, G.A. Omar, Present hydrogeochemistry of the area between El Daba'a and Ras El-Hekma, North Western coast, Egypt, Environmental Science an India Journal, 4-1 (2009) 1-13.

[13] M.A. Khaled, Use of the geoelectrical technique to detect the saline –fresh water interface in the coastal area between Sedi Abd El Rahman–El Dabaa area, Northwestern coast of Egypt, The Egyptian Geophysical Society J. 11-1 (2013) 1-14.

[14] N.A. Morad, M.H. Masoud, S.M. Abdel Moghith, , Hydrologic factors controlling groundwater salinity in the Northwestern coastal zone, Egypt, J. Earth Syst. Sci. 123-7 (2014) 1567–1578.

[15] M. Yousif, R. Geldern, O. Bubenzer, Hydrogeological investigation of shallow aquifers in an arid data-scarce coastal region (El Daba'a, northwestern Egypt), Hydrogeol. J., 24 (2016) 159–179.
[16] Conoco, Geological map of Egypt, scale 1:500,000, GPC, sheets no. NH35NE, Alexandria (1986)
[17] M.Ez. Hilmy, M.M. El Shazly, E.A. Korany, Lithostratigraphy and Petrology of the Miocene and Post-Miocene Sediments in Borg El Arab-El Dabaa Area: Desert Inst. Bull., A.R.E., 28-1 (1978) 1-42.
[18] G.L. Paver, D.A. Pretorious, Report on the reconnaissance hydrogeological investigation in the Western Desert Coastal Zone, Publ. Inst. Desert, Cairo, 1954.
[19] A.K. Abd el-aal, E. Tarabees, H. Badreldin, Source characterization and ground motion modeling computed from the 3 September 2015 Earthquake, Western Desert, Egypt: Int. J. of GEOMATE 12-30 (2017) 160-174.
[20] E. Ibrahim, Geoelectric Resistivity Survey for Site Investigation in East Matruh Area, North Western Desert, Egypt: World Applied Sciences J. 21-7 (2013) 1008-1016.
[21] A. Allam, H. El-Khashab, M. Maamoun, E. Ibrahim, Studies on seismicity in the area of El-Dabaa, Zaafrana and south Safaga nuclear power plant sites, Bull. Helwan Inst. Geophysics (1979) 1-98.
[22] A.A. Hassan, I.M. El Ramly, Preliminary groundwater investigation in Ras El-Hekma area, western Mediterranean Littoral zone, U.A.R. Special report to the Desert Institute, Cairo (1966)
[23] S.M. Atwa, Hydrogeology and Hydrogeochemistry of the North-Western coast of Egypt, Ph.D. Thesis, Fac. Sc., Alexandria Uni. (1979).
[24] A. Salem, A. Hasanein, E. EL Abd, Hydrogeologic setting of El Nigeila area, northwestern coast, Egypt, Egy. J. Geology, 60 (2016) 163-181
[25] U.A. Abu Risha, E.A, El Abd, M.K. Fattah, The role of geology on groundwater evolution in the reclaimed lands to the west of Wadi El Natrun, Egypt, Sedimentology of Egypt, 23 (2017) 93-109.
[26] U.A. Abu Risha, Recharge and evolution of Great Artesian Basin groundwater at Dalhousie, South Australia, PhD thesis, University of South Australia, Adelaide (2010).
[27] D.K. Todd, Ground Water Hydrology, John Wiley and Sons. Inc, 1959.
[28] P.J. Stuyfzand, Predicting the effects of sea spray deposition and evapoconcentration on shallow coastal groundwater salinity under various vegetation types: 23rd Salt Water Intrusion Meeting, June 12-14-2014, Husum, Germany, pp. 401-404.
[29] A.D. Werner, M. Bakker, V.E.A. Post, A. Vandenbohede, C. Lu, B. Ataie-Ashtiani, C.T. Simmons, D.A. Barry Seawater intrusion processes, investigation and management: Recent advances and future challenges, Advances in Water Resources, 51 (2013) 3–26.
[30] S.A., El-Sayed, Contribution to the hydrogeochemistry of groundwater in the Northwest Coastal Plain, Egypt, Isotope and Radiation Research, 42-2 (2010) 293-314.
[31] M.A. Eissa, H.H. Mahmoud, O. Shouakar-Stash, A. El Shiekh, B. Paker, Geophysical and geochemical studies to delineate seawater intrusion in Bagoush area: Northwestern coast, Egypt. J. African Earth Sci., 121 (2016) 365-381.
[32] Y. Gedamy, A. Al-Aassar, M. Amin, E. Shoukry, D. Assy, Hydrochemical Characteristics and Groundwater Quality Assessment for Sustainable Development at Ras El-Hekma Area – Northwestern Coast, Egypt: Current Science International, 6-3 (2017) 589-622.
[33] M. Yousif, T. Oguchi, K. Anazawa, T. Ohba, Geospatial information and environmental isotopes for hydrogeological evaluation: Ras Alam El Rum northwestern coast of Egypt, Nat Resour Res, 23-4 (2014) 423–445.
[34] U. Massoud, M. Soliman, A. Taha, A. Khozym, H. Salah, 1D and 3D inversion of VES data to outline a fresh water zone floating over saline water body at the northwestern coast of Egypt, NRIAG Journal of Astronomy and Geophysics, 4 (2015) 283-292.
[35] M. El Moujabber, B. Bou Samra, T. Darwish, T. Atallah, Comparison of Different Indicators for Groundwater Contamination by Seawater Intrusion on the Lebanese Coast, Water Resources Management, 20-2 (2006) 161–180.
[36] Sudaryanto, W. Naily, Ratio of Major Ions in Groundwater to Determine Saltwater Intrusion in Coastal Areas, IOP Conf. Ser.: Earth Environ. Sci. 118 (2018), 12-21.
[37] IAEA 2018: https://nucleus.iaea.org/wiser/index.aspx
[38] B.R. Scanlon, R.W. Healy, P.G. Cook, Choosing appropriate techniques for quantifying groundwater recharge, Hydrogeology J., 10 (2002) 18–39.
[39] METI and NASA, ASTER GDEM 2 Model, 2011.
[40] A.S. Aliewi, R. Mackay, A. Jayyousi, K. Naserrddin, A. Mushtaha, A. Yaqubi, Numerical Simulation of the Movement of saltwater under skimming and scavenger pumping in the Pleistocene aquifer of Gaza and Jericho areas, Palestine: Transport in porous Media, 43 (2001) 195-212.
[41] A. Kallioras, F.K. Pliakas, C. Schuth, R. Rausch, Methods to Countermeasure the Intrusion of Seawater into Coastal Aquifer Systems, S.K. Sharma, R. Sanghi (eds.), Wastewater Reuse and Management, Springer Science+Business Media Dordrecht, DOI 10.1007/978-94-007-4942-9_17, (2013).
[42] O. Heir, Artificial Recharge of Groundwater with Recycled Municipal Wastewater in the Pajaro Valley: Master's Projects and Capstones, (2016).